Atomic-Physics Tests of QED & the Standard Model

W.R. Johnson
Notre Dame University
http://www.nd.edu/∼johnson

Abstract

A brief review of tests of strong-field QED in many-electron atoms and of atomic parity-nonconservation (PNC) induced by Z_0 exchange is given, with emphasis on the role of precise atomic many-body calculations.

Outline

(1970's) "Strong-Field" Lamb-shift corrections for K-shell electrons in heavy atoms were tested to about 2%.

(Dirac Hartree-Fock level atomic theory)

(1980's) QED corrections for valence electrons in highly-charged Li-like, Na-like, and Cu-like ions were tested to about 5%.

(Third-order relativistic MBPT)

(1990's) Amplitudes for parity-forbidden transitions in Cs, Tl, Bi, and Pb were measured to better than 1%. Comparisons with precise theory in Cs gave a test of the standard-model at the 1% level and the first measurement of a nuclear anapole moment.

(All-order relativistic MBPT)

K-shell Binding Energies

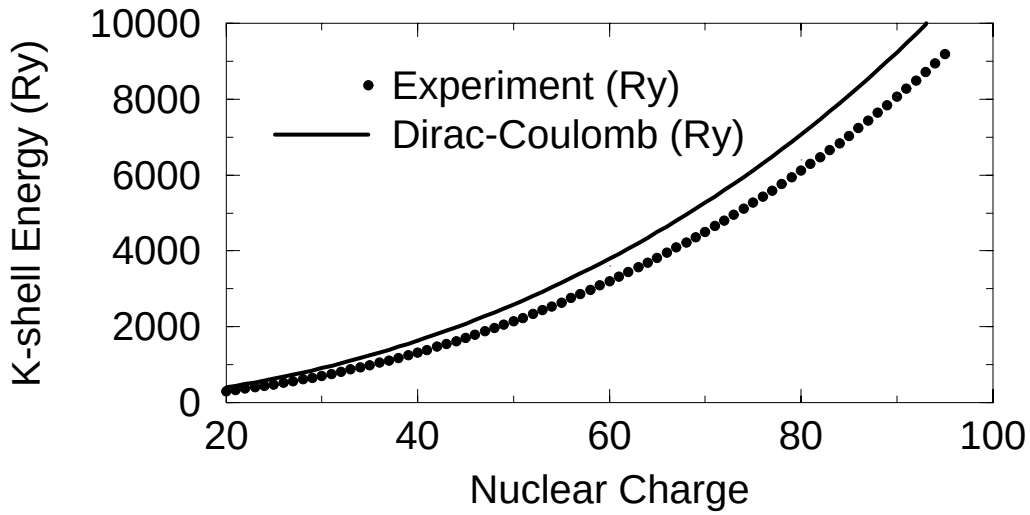

Dirac-Coulomb $1s$ energy

$$\epsilon_{1s} = \frac{2Z^2}{1+\sqrt{1-\alpha^2 Z^2}} \quad \text{Ry}$$

Electron-Electron Interaction

Dirac Hartree-Fock Approximation:

One-electron orbitals ϕ_a satisfy Dirac equations

$$(H_{\rm Dirac} + V_{\rm HF})\phi_a = \epsilon_a \phi_a$$

$$V_{\rm HF}\ \phi_a(\boldsymbol{r}) = \sum_b \int \frac{d^3r'}{|\boldsymbol{r}-\boldsymbol{r}'|}\phi_b^\dagger(\boldsymbol{r}')\phi_b(\boldsymbol{r}')\phi_a(\boldsymbol{r}) - \sum_b \int \frac{d^3r'}{|\boldsymbol{r}-\boldsymbol{r}'|}\phi_b^\dagger(\boldsymbol{r}')\phi_a(\boldsymbol{r}')\phi_b(\boldsymbol{r})$$

Equations solved self-consistently.
$-\epsilon_a =$ "frozen-core" binding energy.

Smaller Corrections

Relaxation Energy:

$$\begin{aligned} E_{1s} =& E_{\rm ion} - E_{\rm atom} \\ =& -\epsilon_{1s} + \Delta_{1s} \end{aligned}$$

Breit Interaction:

$$b_{12} = \frac{\boldsymbol{\alpha}_1 \cdot \boldsymbol{\alpha}_2 + \boldsymbol{\alpha}_1 \cdot \hat{r}_{12}\, \boldsymbol{\alpha}_2 \cdot \hat{r}_{12}}{2r_{12}}$$

Hg $1s$ binding energy (Ry)	
Coulomb	7064.38
HF correction	-911.90
Relaxation	-7.01
Relaxed Breit	-22.29
Breit Retardation	0.45
Nuclear size	-4.03
Structure	6119.59
Expt.	6108.44

Estimated accuracy $\approx$ 0.1 Ry $\approx$ 1 eV

Theory vs. Experiment

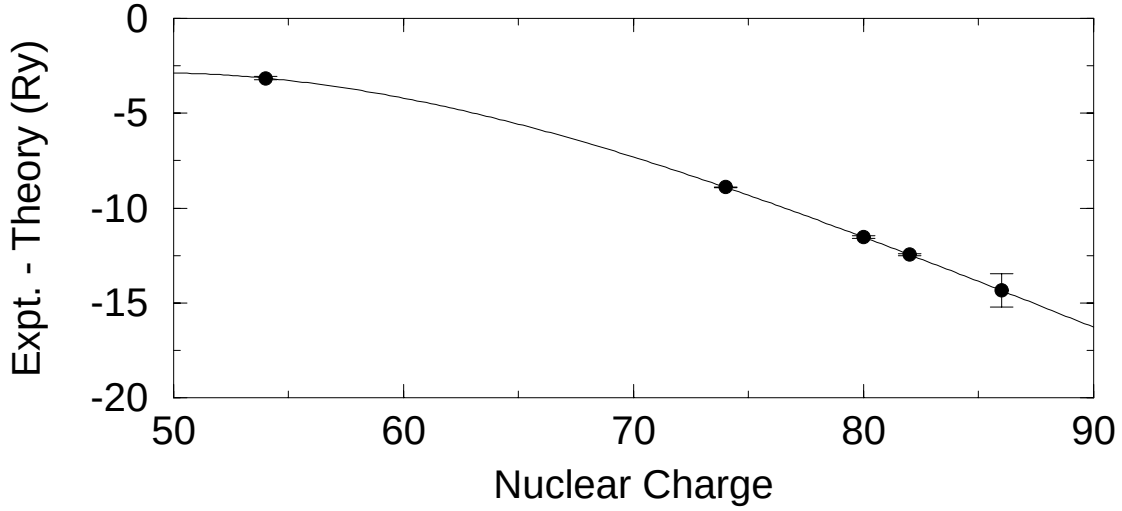

Figure 1: Difference between experimental and theoretical K-shell energies as a function of Z.

K-electron Self-Energy

$$\Delta E_{1s} = \frac{\alpha}{\pi}(\alpha Z)^4 F(Z\alpha) mc^2$$

$$F(Z\alpha) = A_4 + \alpha Z A_5 + (\alpha Z)^2 A_6 + \cdots$$

where,

$$A_4 = \frac{4}{3}\left[\ln(Z\alpha)^{-2} + \frac{5}{6} - 2.9841285\right]$$

$$A_5 = 3\pi\left[1 + \frac{11}{128} - \frac{1}{2}\ln 2\right]$$

$$A_6 = \left[7\ln 2 - \frac{63}{80}\right]\ln(Z\alpha)^{-2} - \frac{3}{4}\ln^2(Z\alpha)^{-2} - 33.2$$

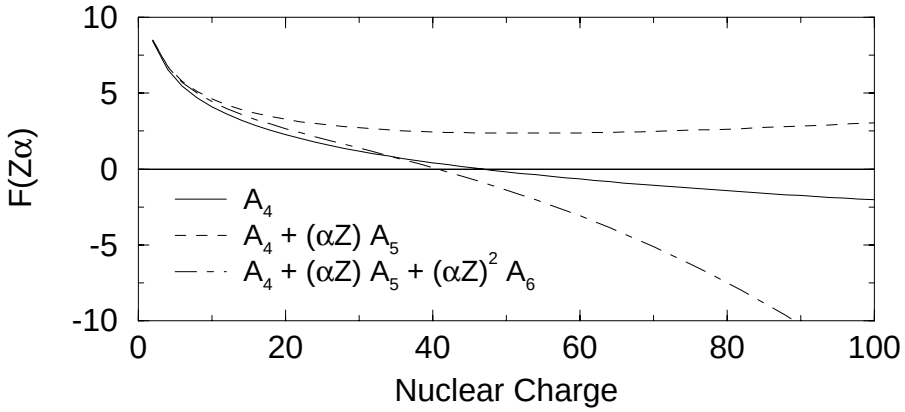

Non-Perturbative $1s$ Self-Energy

- Brown et al. 1959 – $Z = 80$ (incorrect numerics)
- Desiderio 1971 – Coulomb (70 – 90)
- Mohr 1972 – Coulomb (10 – 100)
- Cheng 1976 – Nuclear Size
- Soff et al. 1982 – Nuclear Size
- Blundell & Snyderman 1991
- Lindgren et al. 1993

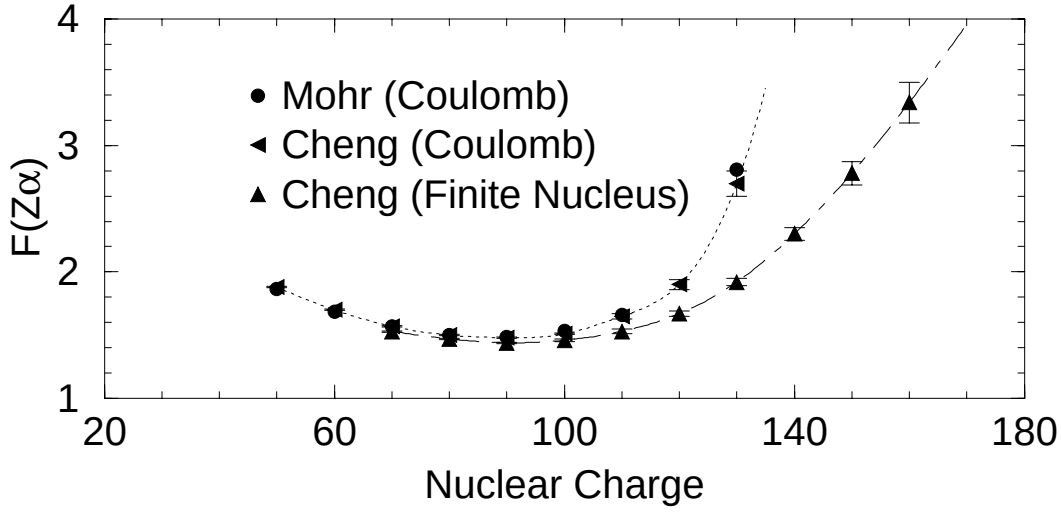

Test of Lowest-Order QED

QED = Self-Energy + Vacuum Polarization
Vacuum-Polarization ≈ Uehling Potential

"Experimental" vs. Theoretical QED

Atom	Expt.	Theory	Diff.	QED
Xe	2540.28(8)	2543.43	-3.15(8)	-3.22
W	5110.42(2)	5119.03	-8.61(2)	-8.73
Hg	6108.44(6)	6119.59	-11.15(6)	-11.36
Pb	6468.71(5)	6480.83	-12.11(5)	-12.35
Rn	7232.73(89)	7247.07	-14.34(89)	-14.51

"Experimental" and Theoretical radiative corrections agree at 2% level of accuracy.

Many-Electron Hamiltonian

The *no-pair* Hamiltonian[1] is a many-electron generalization of the Dirac Hamiltomian derived from the field-theoretic Hamiltonian of QED:

$$H = H_0 + V$$

$$H_0 = \sum_i \epsilon_i \, a_i^\dagger a_i$$

$$V = \frac{1}{2} \sum_{ijkl} v_{ijkl} \, a_i^\dagger a_j^\dagger a_l a_k - \sum_{ij} U_{ij} \, a_i^\dagger a_j$$

1. the sums are restricted to electron states only,

2. v_{ijkl} is a two-particle matrix element of the sum of the Coulomb and Breit interactions,

3. U_{ij} compensates for including $U(r)$ in h_0.

[1] Brown, G.E. & Ravenhall, D.G. 1951 *Proc. R. Soc. London,* Ser. A **208**, 552-559.

QED Tests for Copper-like Ions

Largest atom with a "complete" isoelectronic sequence.

Structure:
$(1s)^2(2s)^2(2p)^6(3s)^2(3p)^6(3d)^{10}$ + valence

Outline of MBPT calculations:

$$E^{(0)} = \sum_a \epsilon_a + \epsilon_v$$

$$E^{(1)} = E_c^{(1)} = -1/2 \sum_a (V_{\rm HF})_{aa}$$

$$E^{(2)} = E_c^{(2)} + E_v^{(2)}$$

$$E^{(3)} = E_c^{(3)} + E_v^{(3)} \quad \cdots$$

$$E_v^{(2)} = \sum_{amn} \frac{\tilde{v}_{mnav} v_{avmn}}{\epsilon_m + \epsilon_n - \epsilon_v - \epsilon_a} - \sum_{abm} \frac{\tilde{v}_{abmv} v_{mvab}}{\epsilon_m + \epsilon_v - \epsilon_a - \epsilon_b}$$

$$E_v^{(3)} = \sum_{mabcd} \frac{\tilde{v}_{abvm} v_{cdab} v_{mvcd}}{(\epsilon_{ab} - \epsilon_{vm})(\epsilon_{cd} - \epsilon_{mv})} + 17 \text{ more terms}$$

Energies of Cu-like Sn (Z=50) (a.u.)

Term	$4s_{1/2}$	$4p_{1/2}$	$4p_{3/2}$
$E^{(0)}$	-23.56930	-21.91682	-21.48453
$E^{(2)}$	-0.06009	-0.06000	-0.05583
$E^{(3)}$	0.00406	0.00383	0.00355
$B^{(1)}$	0.01493	0.02117	0.01478
$B^{(2)}$	-0.00433	-0.00451	-0.00449
$B^{(3)}$	0.00017	0.00027	0.00019
Recoil	0.00009	0.00005	0.00005
$E_{\rm Tot}$	-23.61488	-21.95601	-21.52627

	$p_{3/2} - p_{1/2}$	$p_{3/2} - s_{1/2}$
$E_{\rm Tot}$	0.4297(2)	2.0886(3)
$E_{\rm Expt}$	0.4303(3)	2.0807(1)

Tests of QED in Cu-like Ions

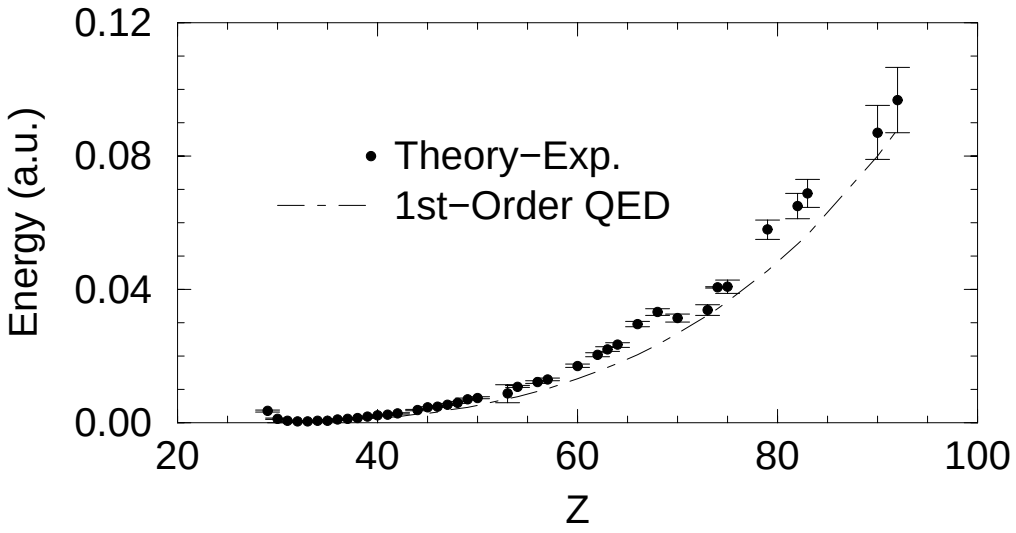

Figure 2: Comparison of "experimental" and theoretical values of the $4p_{3/2} - 4s_{1/2}$ Lamb-shift in copper-like ions.

Conclusion: Calculations of the self-energy and vacuum-polarization corrections carried out in a HF potential agree with "experimental" Lamb-shift to $\sim$ 5% for high-Z Cu-like ions.

Atomic Tests of the Standard Model

$$
\begin{aligned}
H^{(1)} &= \frac{G}{\sqrt{2}}\left(\bar{\psi}_e\gamma_\mu\gamma_5\psi_e\right)\sum_i\Big[c_{1p}\left(\bar{\psi}_{pi}\gamma^\mu\psi_{pi}\right) \\
&\qquad +c_{1n}\left(\bar{\psi}_{ni}\gamma^\mu\psi_{ni}\right)\Big] \\
H^{(2)} &= \frac{G}{\sqrt{2}}\left(\bar{\psi}_e\gamma_\mu\psi_e\right)\sum_i\Big[c_{2p}\left(\bar{\psi}_{pi}\gamma^\mu\gamma_5\psi_{pi}\right) \\
&\qquad +c_{2n}\left(\bar{\psi}_{ni}\gamma^\mu\gamma_5\psi_{ni}\right)\Big]
\end{aligned}
$$

$$
\begin{aligned}
c_{1p} &= \tfrac{1}{2}\left(1-4\sin^2\theta_W\right)\approx 0.038, \\
c_{1n} &= -\tfrac{1}{2}, \\
c_{2p} &= \tfrac{1}{2}\,g_A\left(1-4\sin^2\theta_W\right)\approx 0.047, \\
c_{2n} &= -\tfrac{1}{2}\,g_A\left(1-4\sin^2\theta_W\right)\approx -0.047.
\end{aligned}
$$

$g_A \approx 1.25$ for the partially conserved axial current
$\sin^2\theta_W = 0.23124(24)$ is Weinberg's angle.

Nonrelativistic Nucleon Reduction

$$H^{(1)}_{\rm eff} = \frac{G}{2\sqrt{2}}\,\gamma_5\,Q_w\,\rho(r)$$

$$H^{(2)}_{\rm eff} = -\frac{G}{\sqrt{2}}\,\frac{\kappa-1/2}{I(I+1)}\,\boldsymbol{\alpha}\cdot\mathbf{I}\;\left[c_{2p}\,\rho_{pv}(r)+c_{2n}\,\rho_{nv}(r)\right]$$

$$H^{(a)}_{\rm eff} = \frac{G}{\sqrt{2}}\,K_a\,\frac{\kappa}{I(I+1)}\,\boldsymbol{\alpha}\cdot\mathbf{I}\,\rho_v(r)$$

$$Q_w = \left[\,2\,Z\,c_{1p}+2\,N\,c_{1n}\,\right] = -N+Z\,\left(1-4\sin^2\theta_W\right)$$

Nuclear Anapole

Single-Double Equations

$$\Psi_v = \Psi_{\rm DHF} + \delta\Psi$$

$$\delta\Psi = \left\{ \sum_{am} \rho_{ma}\, a_m^\dagger a_a + \frac{1}{2}\sum_{abmn} \rho_{mnab}\, a_m^\dagger a_n^\dagger a_b a_a \right.$$

$$\left. + \sum_{m\neq v} \rho_{mv}\, a_m^\dagger a_v + \sum_{bmn} \rho_{mnvb}\, a_m^\dagger a_n^\dagger a_b a_v \right\} \Psi_{\rm DHF}$$

$$E_C = E_C^{\rm DHF} + \delta E_C$$

$$E_v = E_v^{\rm DHF} + \delta E_v$$

Later, we will discuss triples

Core Excitation Equations

$$(\epsilon_a - \epsilon_m)\rho_{ma} = \sum_{bn} \tilde{v}_{mban}\rho_{nb}$$
$$+ \sum_{bnr} v_{mbnr}\tilde{\rho}_{nrab} - \sum_{bcn} v_{bcan}\tilde{\rho}_{mnbc}$$

$$(\epsilon_a + \epsilon_b - \epsilon_m - \epsilon_n)\rho_{mnab} = v_{mnab}$$
$$+ \sum_{cd} v_{cdab}\rho_{mncd} + \sum_{rs} v_{mnrs}\rho_{rsab}$$
$$+ \Big[\sum_{r} v_{mnrb}\rho_{ra} - \sum_{c} v_{cnab}\rho_{mc} + \sum_{rc} \tilde{v}_{cnrb}\tilde{\rho}_{mrac}\Big]$$
$$+ \left[\ a \leftrightarrow b \quad m \leftrightarrow n\ \right]$$

$$\delta E_C = \frac{1}{2}\sum_{abmn} v_{abmn}\tilde{\rho}_{mnab}$$

$\approx$ 15,000,000 ρ_{mnab} coefficients for Cs ($\ell = 6$).

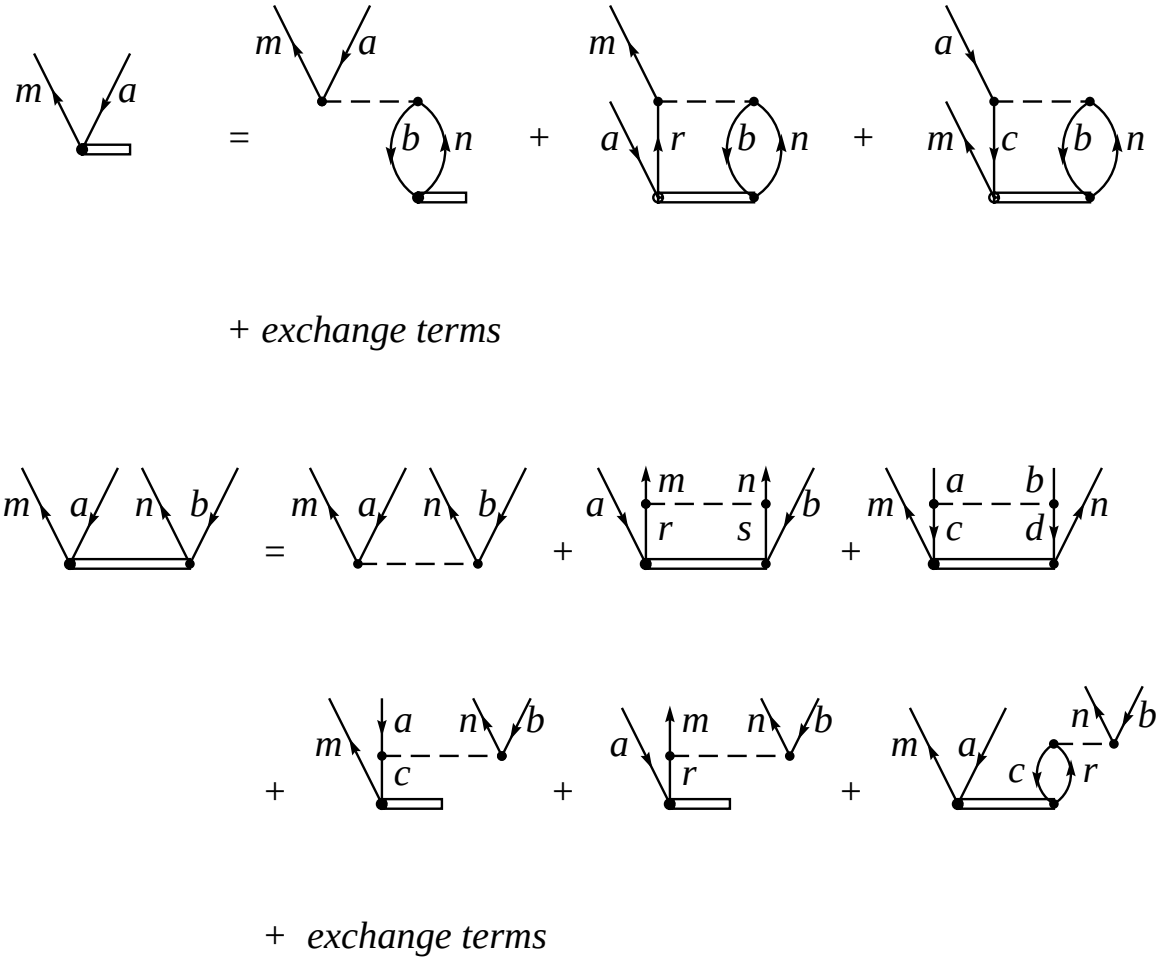

Figure 3: Many-body diagrams for the core SD equations.

Valence Equations

$$(\epsilon_v - \epsilon_m + \delta E_v)\rho_{mv} = \sum_{bn} \tilde{v}_{mbvn}\rho_{nb}$$

$$+ \sum_{bnr} v_{mbnr}\tilde{\rho}_{nrvb} - \sum_{bcn} v_{bcvn}\tilde{\rho}_{mnbc}$$

$$(\epsilon_v + \epsilon_b - \epsilon_m - \epsilon_n + \delta E_v)\rho_{mnvb} = v_{mnvb}$$

$$+ \sum_{cd} v_{cdvb}\rho_{mncd} + \sum_{rs} v_{mnrs}\rho_{rsvb}$$

$$+ \Big[\sum_{r} v_{mnrb}\rho_{rv} - \sum_{c} v_{cnvb}\rho_{mc} + \sum_{rc} \tilde{v}_{cnrb}\tilde{\rho}_{mrvc}\Big]$$

$$+ \left[\ v \leftrightarrow b \quad m \leftrightarrow n\ \right]$$

$$\delta E_v = \sum_{ma} \tilde{v}_{vavm}\rho_{ma} + \sum_{mab} v_{abvm}\tilde{\rho}_{mvab}$$

$$+ \sum_{mna} v_{vbmn}\tilde{\rho}_{mnvb}$$

$\approx$ 1,000,000 ρ_{mnvb} coefficients for each state (Cs)

Perturbation Expansion of the Energy

- δE_C agrees with MBPT through third order.
- δE_v agrees with MBPT through second order.
- $\delta E_v^{(3)}$ disagrees with $E_v^{(3)}$ from MBPT.

Add triple excitations to wave function

$$\frac{1}{6}\sum_{abmnr}\rho_{mnrvab}a_m^\dagger a_n^\dagger a_r^\dagger a_v a_b a_a\,\Psi_{\rm HF}$$

$$E_{v\,\rm extra} = \frac{1}{2}\sum_{mnab}\tilde{v}_{abmn}\rho_{mnvvab}$$

- $\delta E_v^{(3)} + E_{v\,\rm extra}^{(3)}$ gives the entire third-order valence correlation energy

$$E_v^{(3)} = \delta E_v^{(3)} + E_{v\ \mathrm{extra}}^{(3)}$$

Table 1: Na $3s$ and $3p$ states (a.u.)

Term	$3s_{1/2}$	$3p_{1/2}$	$3p_{3/2}$
$\delta E_v^{(3)}$	-3.446[-4]	-1.454[-4]	-1.449[-4]
$E_{v\ \mathrm{extra}}^{(3)}$	-0.418[-4]	-0.070[-4]	-0.072[-4]
$E_v^{(3)}$	-3.865[-4]	-1.525[-4]	-1.521[-4]

Correlation Energy

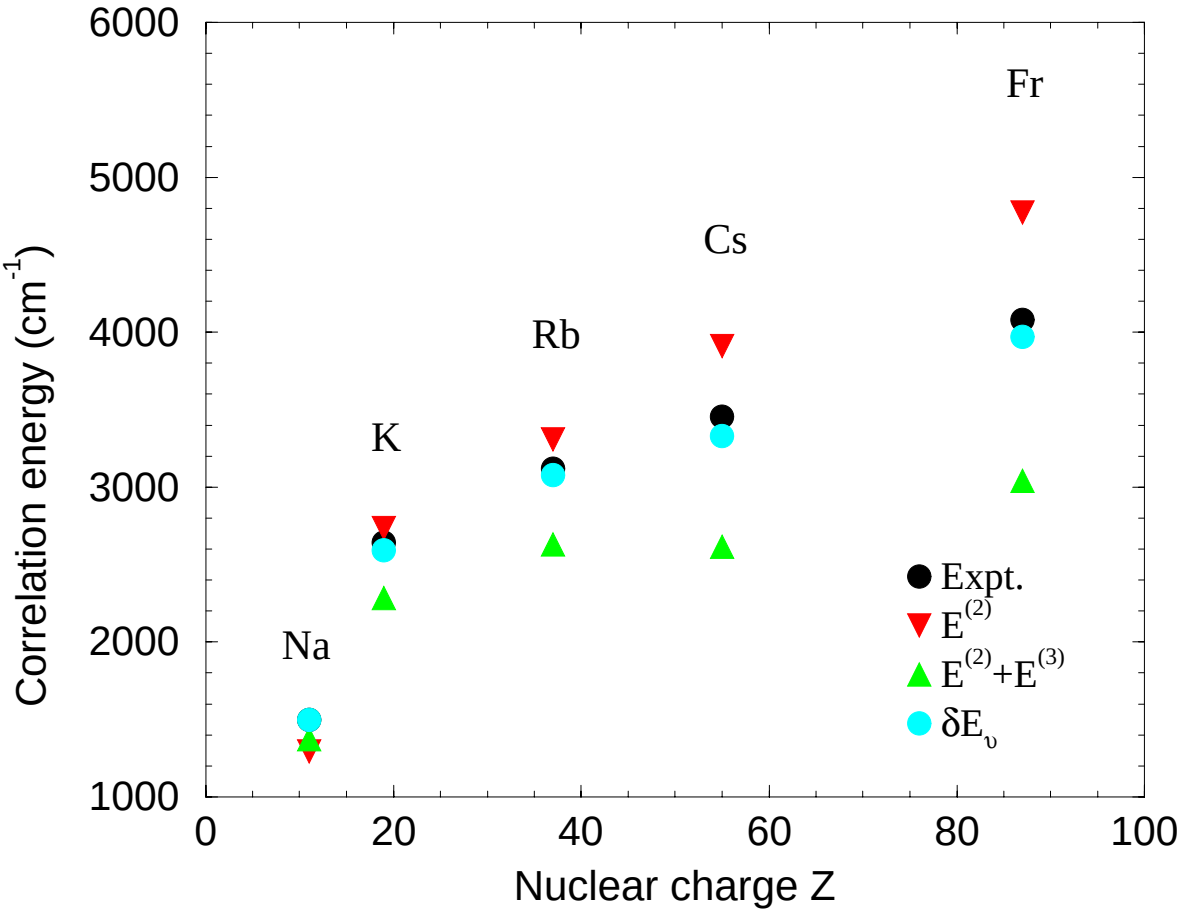

Figure 4: Energy comparisons for alkali-metal atoms.

Higher-order terms

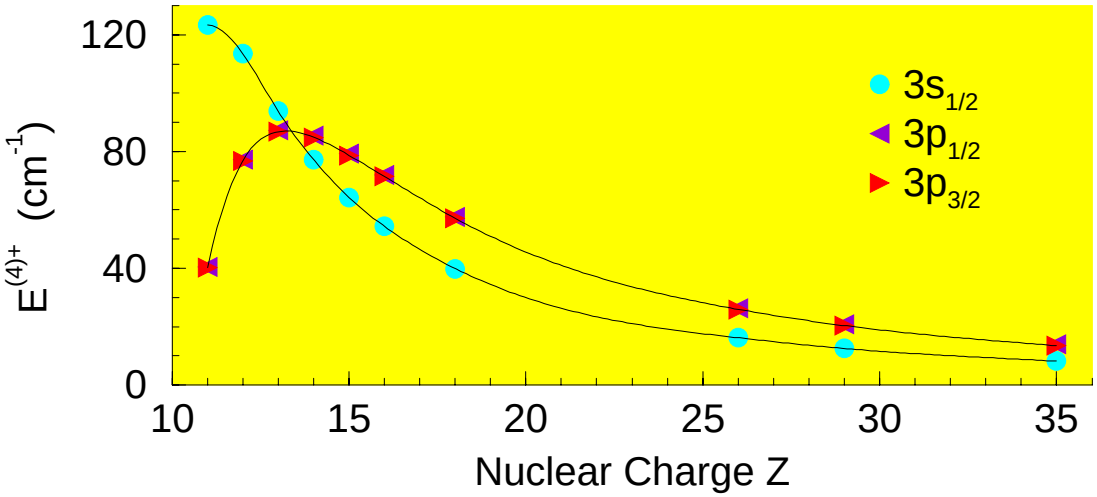

Figure 5: Contributions beyond 3rd-order for Na-like ions.

- $E^{(4)+} < 1\%$ of correlation energy for $Z > 20$

All-order energies

Table 2: Summary for sodium $3s$ and $3p$ states (cm^{-1})

Term	$3s$	$3p_{1/2}$	$3p_{3/2}$
DHF	-39951.6	-24030.4	-24014.1
δE	-1488.8(4)	-463.9	-461.6
$E^{(3)}_{\mathrm{extra}}$	-9.2	-1.5	-1.6
Breit	1.2	1.4	0.1
RM+MP	1.0	0.5	0.5
Theory	-41447.3(4)	-24493.9	-24476.7
Expt.	-41449.4	-24493.3	-24476.1

Results for Heavy Atoms

Table 3: Energies for cesium and francium cm^{-1}

Cs	$6s$	$7s$	$8s$	$9s$
Theory	31262	12801	7060	4479
Expt.	31407	12871	7089	4496
Cs	$6p_{1/2}$	$7p_{1/2}$	$8p_{1/2}$	$9p_{1/2}$
Theory	20204	9621	5687	3760
Expt.	20228	9641	5698	3769
Fr	$7s$	$8s$	$9s$	$10s$
Theory	32735	13051	7148	4522
Expt.	32849	13106	7168	4538
Fr	$7p_{1/2}$	$8p_{1/2}$	$9p_{1/2}$	$10p_{1/2}$
Theory	20583	9712	5724	3782
Expt.	20612	9736	*5738*	*3795*

Fine-Structure Intervals

Table 4: Fine-structure (cm^{-1}).

		This work	Expt.
K	$4p_{3/2} - 4p_{1/2}$	57.3	57.7
	$5p_{3/2} - 5p_{1/2}$	18.5	18.8
	$6p_{3/2} - 6p_{1/2}$	8.5	8.4
	$7p_{3/2} - 7p_{1/2}$	4.4	4.5
Rb	$5p_{3/2} - 5p_{1/2}$	236.5	237.6
	$6p_{3/2} - 6p_{1/2}$	76.5	77.5
	$7p_{3/2} - 7p_{1/2}$	34.8	35.1
	$8p_{3/2} - 8p_{1/2}$	18.6	18.9
Cs	$6p_{3/2} - 6p_{1/2}$	552.2	554.1
	$7p_{3/2} - 7p_{1/2}$	178.6	181.0
	$8p_{3/2} - 8p_{1/2}$	81.4	82.6
	$9p_{3/2} - 9p_{1/2}$	43.9	44.7
Fr	$7p_{3/2} - 7p_{1/2}$	1676	1687
	$8p_{3/2} - 8p_{1/2}$	536	545
	$9p_{3/2} - 9p_{1/2}$	244	*250*
	$10p_{3/2} - 10p_{1/2}$	132	*136*

Dipole Transitions

Table 5: Matrix Elements for heavy alkali metals (a.u.)

	K	Rb	Cs	Fr
$p_{1/2}$–s	$n=4$	$n=5$	$n=6$	$n=7$
SD	4.098	4.221	4.478	4.256
Expt.	4.102(5)	4.231(3)	4.489(7)	4.277(8)
$p_{3/2}$–s	$n=4$	$n=5$	$n=6$	$n=7$
SD	5.794	5.956	6.298	5.851
Expt.	5.800(8)	5.977(4)	6.324(7)	5.898(15)

Application to PNC

$$\begin{aligned}\langle F|ez|I\rangle &= \sum_n \frac{\langle F|ez|n\rangle\langle n|H_W|I\rangle}{E_n - E_I} \\ &+ \sum_n \frac{\langle F|H_W|n\rangle\langle n|ez|I\rangle}{E_n - E_F},\end{aligned}$$

where $H_W = H_{\rm eff}^{(1)} + H_{\rm eff}^{(2)} + H_{\rm eff}^{(a)}$

$$\langle F|ez|I\rangle = E_{\rm PNC}\,[1 + A(F_F, F_I)]$$

For ^{133}Cs ($I = 7/2$), we obtain:

$$E_{\rm PNC} = 0.906(9)\ \times 10^{-11}\, i|e|a_0 Q_w/N$$

$$A(F_F,\, F_I) = \begin{bmatrix} 0.028 & 0.057 \\ -0.051 & -0.022 \end{bmatrix}$$

Status of PNC Experiments

(a) Optical rotation: $n_+ \neq n_-$ $\quad \phi = E_{\rm PNC}/M_1$

$6p_{1/2} - 6p_{3/2}$ transition

Element	Group	$10^8 \times \phi$
Thallium	Oxford	-15.7(5)
Thallium	Seattle	-14.7(2)
Lead	Oxford	-9.8(1)
Lead	Seattle	-9.9(1)
Bismuth	Oxford	-10.1(20)

(b) Stark interference: Add $E(t) = A\cos\omega t$ and detect the hetrodyning signal R $= E_{\rm PNC}/\beta$

$6s_{1/2} - 7s_{1/2}$ (mV/cm)

Element	Group	R_{4-3}	R_{3-4}
Cesium	Paris (1984)	-1.5(2)	-1.5(2)
Cesium	Boulder (1988)	-1.64(5)	-1.51(5)
Cesium	Boulder (1997)	-1.635(8)	-1.558(8)

Cesium: Theory vs. Experiment

$\beta = 27.02(8)\, a_0^3$ (1999)

(eliminating axial vector + anapole contribution)

$\Im(E_{\rm PNC}) = -0.836(4) \times 10^{-11}|e|a_0$ (1997)

(dividing by theoretical matrix element)

$Q_w = -71.9(4)$ (Expt.+ Atomic Theory)

$K = 0.50(7)$ (Expt.+ Atomic Theory)

Marciano & Rosner (with radiative corrections)

$Q_w = -73.20(13)$ (Standard Model)

Expt. - Theory = 1.3(4)

Principal source of error is atomic theory.

Conclusions

I Strong-field QED corrections inner-shell electrons in heavy atoms are tested to 2%.

II Comparing theoretical and "experimental" values of the Lamb-shift for valence electrons in highly-charged ions provide stringent tests of higher-order MBPT calculations.

III Tests of the standard-model by comparing experiment and theory show a $\sim 3\sigma$ effect in Q_w.

IV Modern atomic PNC experiments are underway at Stonybrook, Berkeley, and Seattle. Calculations are needed to aid in extracting quantitive information from such measurements.